Journal of Renewable Materials

Tech Science Press

DOI: 10.32604/jrm.2023.025126

check for updates

ARTICLE

Preparation and Properties of Vegetable-Oil-Based Thioether Polyol and Ethyl Cellulose Supramolecular Composite Films

Ruyu Yan[1,2,3,4], Jian Fang[1,*], Xiaohua Yang[2,3,4,5,6], Na Yao[2,3,4,5,6], Mei Li[2,3,4,5,6], Yuan Nie[2,3,4,5,6], Tianxiang Deng[2,3,4,5,6], Haiyang Ding[2,3,4,5,6], Lina Xu[2,3,4,5,6] and Shouhai Li[2,3,4,5,6,*]

[1]College of Materials Science and Technology, Beijing Forestry University, Beijing, 100083, China

[2]Institute of Chemical Industry of Forestry Products, CFA, Nanjing, 210042, China

[3]National Engineering Lab. for Biomass Chemical Utilization, Nanjing, 210042, China

[4]Key Lab. of Chemical Engineering of Forest Products, National Forestry and Grassland Administration, Nanjing, 210042, China

[5]Key Lab. of Biomass Energy and Material, Nanjing, 210042, China

[6]Jiangsu Co-Innovation Center of Efficient Processing and Utilization of Forest Resources, Nanjing, 210042, China

[*]Corresponding Authors: Jian Fang. Email: fj515@sina.com; Shouhai Li. Email: lishouhai1979@163.com

Received: 23 June 2022 Accepted: 04 August 2022

ABSTRACT

Ethyl cellulose (EC), an important biomass-based material, has excellent film-forming properties. Nevertheless, the high interchain hydrogen bond interaction leads to a high glass transition temperature of EC, which makes it too brittle to be used widely. The hydroxyl group on EC can form a supramolecular system in the form of a non-covalent bond with an effective plasticizer. In this study, an important vegetable-oil-based derivative named dimer fatty acid was used to prepare a novel special plasticizer for EC. Dimer-fatty-acid-based thioether polyol (DATP) was synthesized and used to modify ethyl cellulose films. The supramolecular composite films of DATP and ethyl cellulose were designed using the newly-formed van der Waals force. The thermal stability, morphology, hydrophilicity, and mechanical properties of the composite films were all tested. Pure EC is fragile, and the addition of DATP makes the ethyl cellulose films more flexible. The elongation at the break of EC supramolecular films increased and the tensile strength decreased with the increasing DATP content. The elongation at the break of EC/DATP (60/40) and EC/DATP (50/50) was up to 40.3% and 43.4%, respectively. Noticeably, the thermal initial degradation temperature of the film with 10% DATP is higher than that of pure EC, which may be attributed to the formation of a better supramolecular system in this composite film. The application of bio-based material (EC) is environmentally friendly, and the novel DATP can be used as a special and effective plasticizer to prepare flexible EC films, making it more widely used in energy, chemical industry, materials, agriculture, medicine, and other fields.

KEYWORDS

Ethyl cellulose; dimeric fatty acid based thioether polyol; supramolecular system; composite films

1 Introduction

Film materials play an increasingly important role in life and industrial production following the development of society. However, most of the films originated from petroleum and coal chemical products, and these fossil resources are facing the risk of depletion [1]. Meanwhile, most of these fossil-

based films cannot be recycled or naturally degraded, so the waste film materials will severely threaten the environment [2,3]. In pace with people's improved awareness of environmental protection and resource preservation, the development of renewable resources-based films has attracted great attention [4–7].

Starch, cellulose, chitosan, vegetable oil, and their derivatives are commonly-used raw materials for preparing biomass-derived products, including films. These renewable biomass resources, which are highly potential to replace traditional petrochemical products in daily life and industrial fields, have gained extensive attention [8–10].

As the most widely-sourced natural resource, cellulose has generated a large number of derivatives and is used in medicine, coatings, membrane technology, construction, and other fields. For example, bacterial cellulose (BC), which is usually used as a wound dressing for repairing human skin and tissue, is characterized by good biocompatibility, adaptability, and air permeability [11]. Zhao developed a stiffness-changing material composed of cellulose (Cel) and PAA, the biomimetic Cel–PAAm has a unique self-healing behavior and a self-regulating capability between soft state and reinforced state [12]. Ethyl cellulose (EC), an important cellulose derivative, has high plasticity, biocompatibility, and heat and light resistance [13–16]. Remarkably, EC possesses excellent film-forming performance like other cellulose derivatives [17–20]. However, the brittleness of EC films restricts their applications in many fields. Consequently, plasticizers are needed as additives to strengthen the flexibility and processability of EC films [21,22]. Some petroleum-based plasticizers of EC films include dibutyl sebacate, citrate, triacetate, triethylacetylated monoglyceride, and diethyl phthalate [23,24], but the effect on improving the performance of ethyl cellulose films is not significant [25]. In addition, owing to toxicity, most petroleum-based plasticizers are strictly forbidden in medicine and children's products. Thus, many eco-friendly bio-based plasticizers are continuously explored for sustainable development. Triethyl citrate (TEC) can considerably enhance flexibility and reduce the glass transition temperature of EC films. Additionally, many common plasticizers such as dioctyl-phthalate (DOP), dioctyl terephthalate, and bio-based TEC were used to plasticize EC materials. They can easily migrate out from composite films without forming supramolecular systems with EC. Therefore, high-efficiency and low-toxicity plasticizers shall be prepared and used to form supramolecular systems with EC.

Noncovalent bonds (e.g., hydrogen bonds, metal coordination, hydrophobic or hydrophilic bonds, π-π interactions, van der Waals forces) can construct supramolecular systems [26]. Ethyl cellulose, an amphiphilic polymer, can form many hydrogen bonds as well as hydrophobic or hydrophilic interactions, and easily form supramolecular systems. Li et al. synthesized and used a new type of ricinoleic acid mercaptotriol (STRA) to plasticize EC films [27]. A series of composite films with different proportions of STRA and EC based on van der Waals forces were prepared, and their flexibility and hydrophilicity were improved to a certain extent. Lin combined bio-based small-molecule lipoic acid (LA) and EC to produce supramolecular composite films [28]. LA weakened the hydrogen bond and hydrophobic binding in EC molecular chains, which remarkably improved the flexibility and processability of ethyl cellulose films. When the LA content was 20%−50%, the elongation at break of EC composite films rose by 5.5–11.1 times.

Dimer fatty acid is a widely-used vegetable-oil-based derivative, which molecularly contains two carboxyl groups, more than one unsaturated double bond, and long fat chains. It can be used to prepare many chemical products. Lee prepared dimer acid (DA) esters with different short to long alkyl chains via the hydrolysis of waste vegetable oil, Diels-Alder reaction, and esterification of fatty acids [21]. The DA esters had higher thermal stability than DOP, a petroleum-based plasticizer. The optical clarity and SEM images of the composite films composed of DA esters and EC showed high miscibility on a micro-scale [29].

In this study, the method to synthesize a novel bio-based thioether polyol plasticizer from dimer fatty acid was first introduced. Thus, the plasticizer was named dimer-fatty-acid-based thioether polyol (DATP). Then various supramolecular films of EC and DATP were prepared. The thioether group and hydroxyl group in DATP can be combined with the hydroxyl group of EC when composite systems are

regenerated [30]. The morphology, hydrophilicity, thermal stability, and mechanical properties of the composite films were all tested. This study provides a distinct guide for the preparation of such materials.

2 Experimental

2.1 Raw Materials

NaOH (AR, 97.0%), and benzyl triethyl ammonium chloride (98%) were obtained from Aladdin Industrial Co., Ltd., China. Dimer fatty acids (stabilized, 91.5%) were provided by Jiangxi Yichun Yuanda Chemical Industry Co., Ltd., China. The epichlorohydrin (AR, ≥99.0%) was purchased from Shanghai Lingfeng Chemical Reagent Co., Ltd., China), the diatomaceous earth (Shanghai Aladdin Biochemical Technology Co., Ltd., China), acetic acid (≥99.5%, Chinasun Specialty Products Co., Ltd., China), and mercaptoethanol (AR, 99%, Xiya Reagent, China). Ethyl cellulose M70 (EC, CP) was provided by the Sinopharm Chemical Reagent Co., Ltd., China. Calcium oxide (Xilong Chemical Company, China). All materials were used as received without further purification.

2.2 Synthesis of Dimer-Fatty-Acid-Based Thioether Polyol

Dimer-fatty-acid-based epoxy (DAE) resulted from dimer fatty acid and epichlorohydrin by ring-opening and the closing reaction of epoxy groups and then was converted to the DATP. Scheme 1 displays the synthesis of DATP.

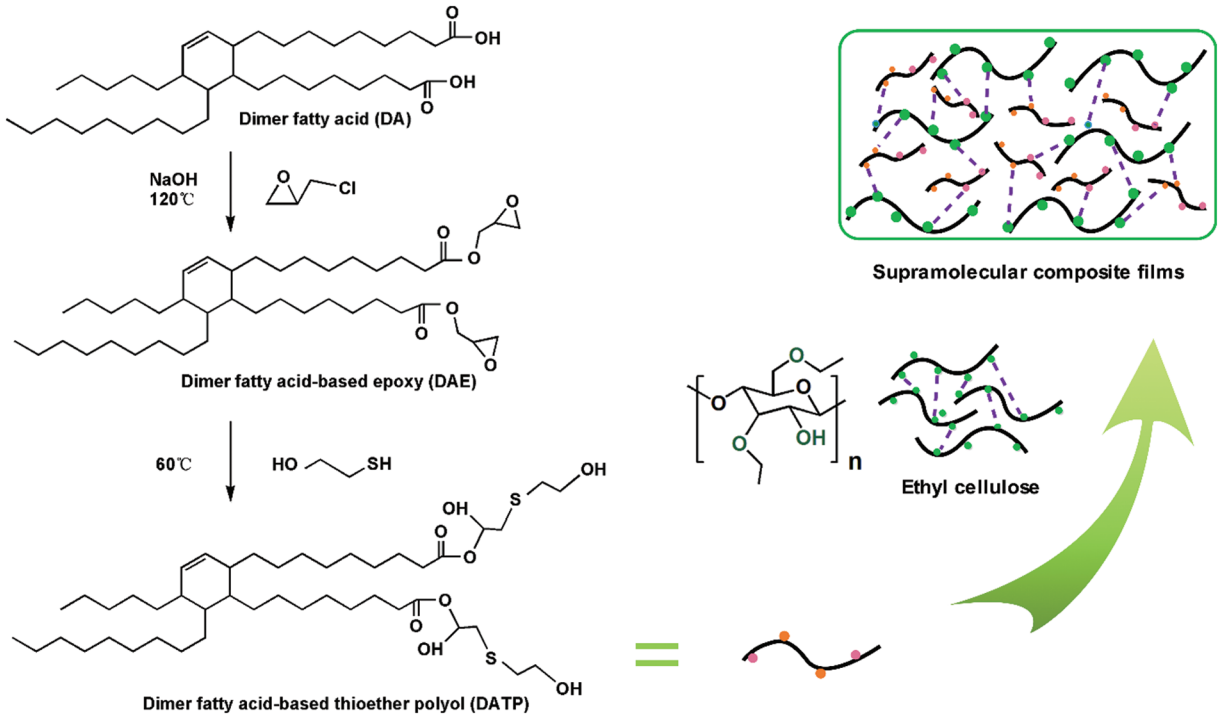

Scheme 1: Synthetic route of DATP and films of EC and DATP

Firstly, 84.15 g (0.15 mol) of dimer fatty acid, 139.50 g of epichlorohydrin, and 1.40 g of benzyl trimethyl ammonium chloride were put into a 500 mL flask containing a magnetic stirrer, a thermometer, and a reflux condenser. Then the mixed reactants were heated to 100°C and held for 3 h. After cooling to 60°C, 12.00 g (0.3 mol) of NaOH and 16.80 g (0.3 mol) of CaO were added under stirring for 3 h. After

the reaction, the product was filtered with a Buchner funnel covered with diatomite, and the filtrate was collected. A light orange viscous liquid DAE was formed after excessive epichlorohydrin was distilled via rotary vacuum evaporation. The epoxy value of DAE was 0.241 mol/100 g.

Then 10.00 g of DAE, 1.76 g of mercaptoethanol, and 0.12 g of DMP-30 were added to a 100 mL flask containing the three devices mentioned above. After stirring at 120°C and 400 r/min for 2 h, DATP was obtained.

2.3 Preparation of the EC and DATP Composite Films

Scheme 1 plots the two-step synthesis of EC composite films. First, EC was dissolved in acetic acid and stirred at 80°C for 1 h to form 7.3% (w/w) solutions. Second, supramolecular composite films with different DATP contents were made by casting (the preferred method to prepare films). DATP was blended with the 7.3% EC solutions and stirred at 80°C for 0.5 h. Next, the solution was removed into a clean polypropylene mold with a casting area of 70 × 100 mm^2 and dried at 120°C for 2 h. Films containing 0, 10, 20, 30, 40, or 50 wt% DATP were obtained and named as EC/DATP (*x*) (*x* = 100/0, 90/10, 80/20, 70/30, 60/40, 50/50, respectively). The compositions of EC/DATP are listed in Table 1.

Table 1: Formulation of EC composite membranes with different proportion

Formulations	DATP (g)	EC (g)	EC acetic acid solution 7.3% (w/w) (g)
EC/DATP (90/10)	0.25	2.25	33.07
EC/DATP (80/20)	0.50	2.00	29.40
EC/DATP (70/30)	1.00	2.33	34.30
EC/DATP (60/40)	1.00	1.50	22.05
EC/DATP (50/50)	1.00	1.00	14.70

2.4 Characterization

2.4.1 Epoxy Value

The epoxy values were characterized according to Chinese Standards GB/T 1677-2008 and calculated by the following formula: $EPV = \frac{(V_o - V) \times C}{10 \times w}$

V_0: volume of standard sodium hydroxide solution consumed in blank test (57.10 ml)

V: volume of standard sodium hydroxide solution consumed by the sample (42.40 ml)

C: concentration of sodium hydroxide standard solution (0.0984 mol/L)

W: sample quality (0.600 g)

2.4.2 Nuclear Magnetic Resonance (^1H NMR)

The ^1H NMR of DA, DAE, and DATP were recorded using an AVANCE III HD 400 MHz spectrometer at room temperature, $CDCl_3$ was employed as a deuterated solvent.

2.4.3 Attenuated Total Reflectance–Fourier Transform Infrared Spectroscopy (ATR-FTIR)

The ATR-FTIR of DA, DAE, DATP, and composite films were recorded by Nicolet IS10 spectrometer (Thermo-fisher, USA). Each sample was recorded in the range of 4000–500 cm^{-1} at a resolution of 4 cm^{-1}.

2.4.4 Scanning Electron Microscope (SEM)

The micrographs of the supramolecular composite films were scanned by Hitachi S3400-N (Japan). For the sake of avoiding electrostatic charging during the examination, the exposed fracture surface cryofractured by liquid nitrogen was coated with gold.

2.4.5 Thermal Gravimetric Analysis (TGA)

A NETZSCH STA 409 PC (Netzsch Instrument Crop., Germany) was used to perform TGA tests. The samples were heated from 40°C to 800°C under a nitrogen atmosphere at a rate of 15 °C/min.

2.4.6 Dynamic Mechanical Analysis (DMA)

A dynamic mechanical analyzer (Rheometric Scientific IV) with stretching mode at an oscillatory frequency of 1 Hz was employed for DMA testing. The DMA test specimens with a size of approximately 40.0 mm (L) × 6.0 mm (W) × 0.3 mm (T) were cut with a utility knife. The measurements were carried out at a heating and cooling rate of 3 °C/min from −80°C to 60°C in a liquid N_2 atmosphere.

2.4.7 Mechanical Properties

Tensile properties of the samples were measured by an E43.104 Universal Testing Machine (MTS Instrument Crop., China) with a crosshead speed of 5 mm/min. The test of tensile strength and elongation at break is in the light of GB/T 1040-2006 (China). The dumbbell-shaped samples for tensile tests were obtained by a manual punching machine (Yangzhou Yuanfeng Testing Equipment Co., Ltd., China), and the specimens' size was approximately 50.0 mm (L) × 4.0 mm (W) × 0.3 mm (T). Under a fixed test temperature of 25°C, five specimens were tested at a crosshead speed of 5 mm/min, and the average values were obtained.

2.4.8 Water and Oil Contact Angle

The water and oil contact angles of EC films were tested by instrument (DSA 100, Krüss, Hamburg, DE) to evaluate the hydrophilicity of EC films. 5 μL of water and oil were separately dripped on the film surface and stabilized for 60 s, all measurements were carried out at 20°C, and the final water and oil contact angle values are the average value of three replicates.

3 Results and Discussion

3.1 FTIR and ^{1}H NMR of DA, DAE, and DATP

ATR-FTIR spectra of DA, DAE, and DATP are shown in Fig. 1a. There are two identical characteristic peaks in all three spectra. The peaks at 2921 and 2852 cm^{-1} confirm the presence of methyl and methylene groups, respectively. The peak around 1706 cm^{-1} is attributed to the carboxyl group, which fully disappeared in other spectra.

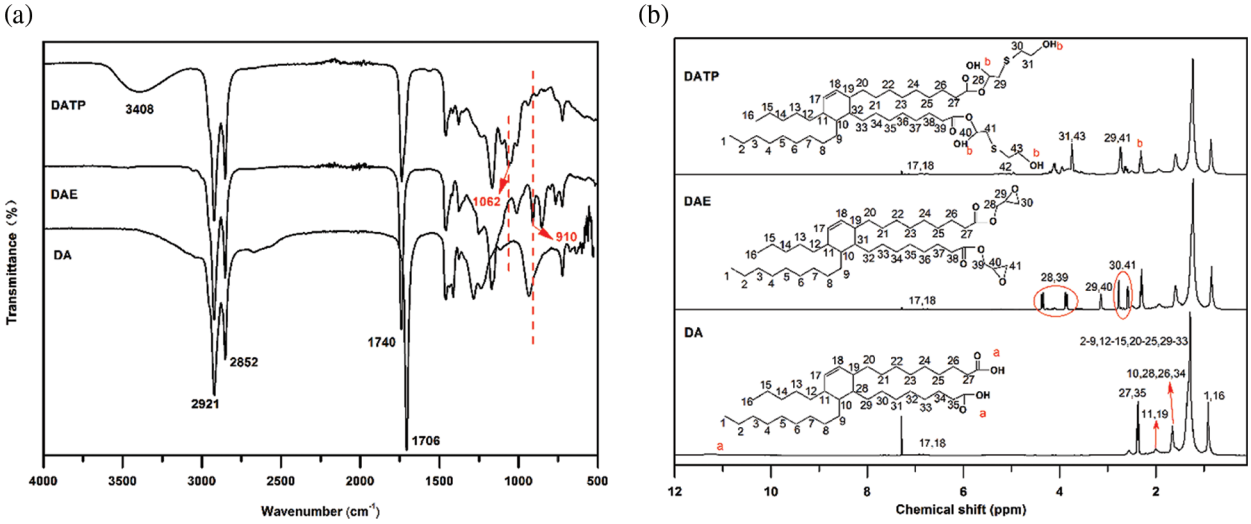

Figure 1: FTIR and ^{1}H NMR spectra of DA, DAE and DATP

In comparison with the spectrum of DA, the peak at 910 cm^{-1} corresponds to the epoxy group, and the ester group peak at 1740 cm^{-1} exists in DAE. The FTIR above suggests the successful epoxidation of DA. In the FTIR spectrum of DATP, the peak of the epoxy group is almost absent and two new peaks caused by primary hydroxyl appear at 3408 and 1062 cm^{-1}. These results demonstrate the successful reaction between S-H and the epoxy groups. All the FTIR spectra indicate the successful synthesis of DATP.

Fig. 1b exhibits the ^{1}H-NMR spectra of DA, DAE, and DATP, with detailed attributions of chemical shifts of protons. On the DA spectrum, the peak around 11.3 ppm corresponds to the hydroxy of the carboxyl group, which is almost absent in DAE. Besides, new peaks at 2.5−2.8 ppm, 3.1 ppm, and 3.8 −4.4 ppm in the ^{1}H-NMR spectrum of DAE are ascribed to the epoxy group. Compared with the ^{1}H-NMR spectrum of DAE, the peak standing for the proton of CH-O-CH_2 around 3.0 ppm is fully unseen on the spectrum of DATP. Moreover, the peak at about 2.3 ppm indicates the presence of the hydroxy group, and the peaks at 2.6−2.7 ppm ascribed to the proton of −S−CH_2− are weakened. All these ^{1}H-NMR spectra prove the successful synthesis of DATP [31].

3.2 FTIR of EC and EC/DATP Films

Fig. 2 depicts the FTIR spectra of supramolecular EC composite films with varying proportions of DATP. The pure EC film shows distinct peaks at around 3474 and 1051 cm^{-1}, which represent O-H and C-O-C stretching, respectively. With the addition of DATP, the new peak at 1738 cm^{-1} ascribed to the carbonyl group appeared. In addition, as can be seen from the FTIR spectra of different EC films, the peaks (3474–3459 cm^{-1}) belonging to the stretching vibration of O-H shifted to lower frequency and the width of which increased, due to the formation of hydrogen bonds between DATP and ethyl cellulose, and the force constant lowering in the bound state [32]. Therefore, it can be observed that good supramolecular systems were formed by DATP and EC.

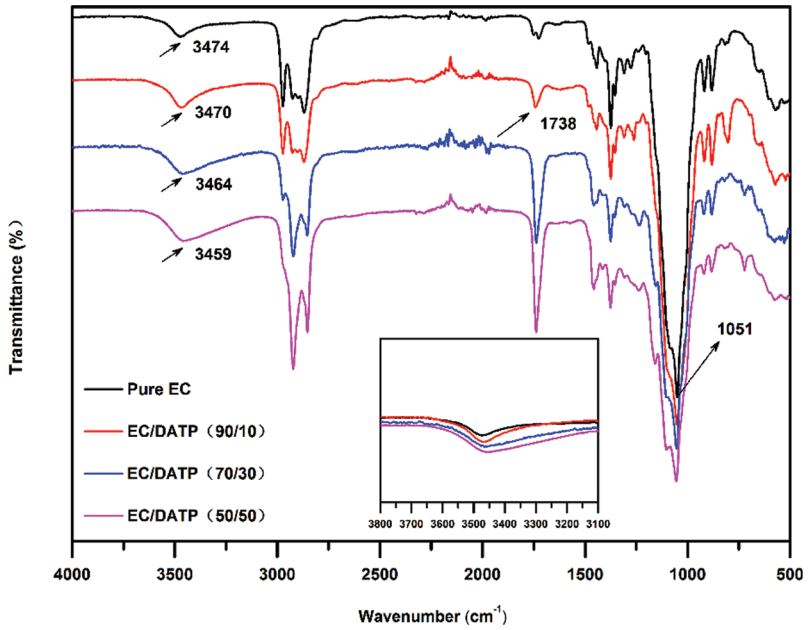

Figure 2: ATR-FTIR spectra of different EC films

3.3 Morphology of EC and EC/DATP Films

The photos of EC films on the black paper are shown in Fig. 3. We can see that the EC films are relatively transparent compared with pure EC, indicating that EC and DATP are very compatible. Pure EC film is very brittle and divided into two parts when it bends. EC films with DATP remain intact when bent by tweezers. DATP can improve the flexibility of EC film to some extent.

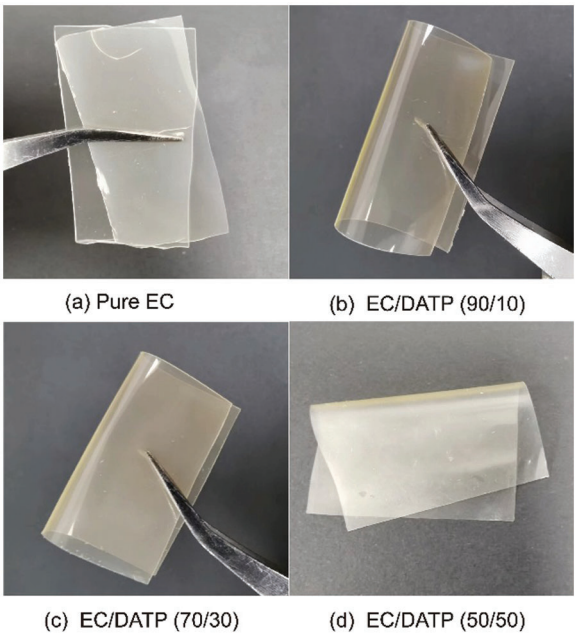

Figure 3: Photos of EC films

Fig. 4 displays the SEM images of the films at the exposed section (magnification 2000 and 5000 times). Many holes exist on the fractured surface of pure EC film, owing to the relatively poor hydrogen bonding system caused by the large steric hindrance of EC molecules. With more DATP added to the EC films, fewer holes appear on the cross-section of EC composite films. When there are a lot of holes on the fracture surface of the film, it is brittle. With the addition of DATP, the surface presents a lamellar structure, which indicates that the flexibility of the film has been improved, when the surface is relatively smooth, the flexibility of the film is best. Hence, DATP can be well embedded into EC molecular chains to form novel supramolecular systems through hydrogen bonding.

3.4 TGA

TGA was used to evaluate the thermal stability of different EC films. The thermal data of special temperatures with 5%, 10%, and 50% mass losses (marked T_5, T_{10}, and T_{50} respectively), the fastest decomposition temperature T_{max} and carbon yield at 600°C (CY600) of EC films were listed in Table 2. The thermal degradation curves of composite films are exhibited in Fig. 5. Apparently, the initial thermal degradation of pure EC (T_5) occurred at 301.2°C, but dropped to 293.7°C and 276.3°C in the composite films with 30% and 50% DATP, respectively. The reason is that heat destroys the van der Waals interactions [31] so DATP molecules are released from the composite films during the heating. Significantly, the initial degradation temperature of the composite film with 10% DATP is higher than that of pure EC, which may result from a better supramolecular system formed in this composite film. Thermal degradation of EC started at 300°C and ended at 390°C. For composite films, major

decomposition occurred within 320°C–380°C, which was related to the thermal degradation of EC. When at above 380°C, the weight percentages of all composite films were higher than that of pure EC, which means relatively higher thermal stability of composite films. This evidence suggests that DATP can be used as an effective additive to maintain thermal stability for EC films.

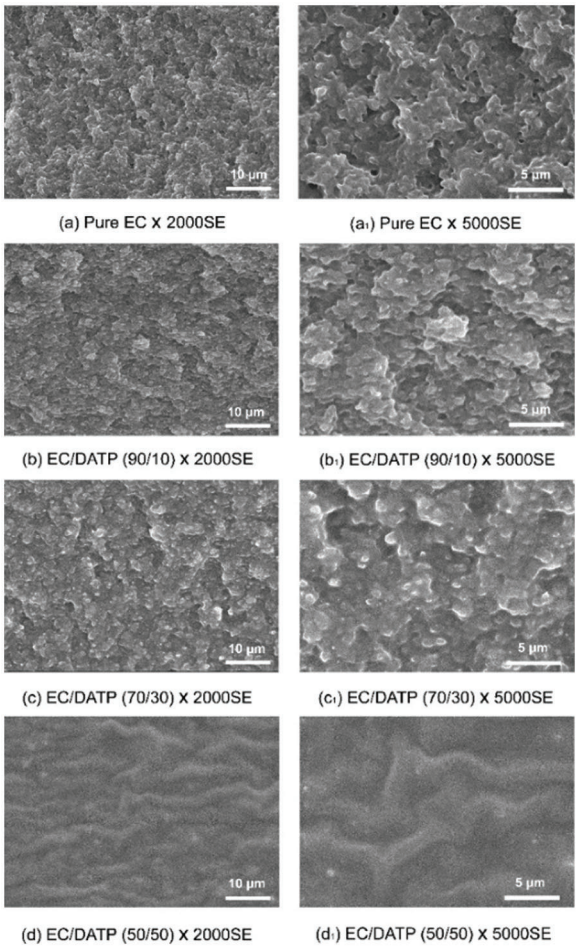

Figure 4: SEM images of fractured surface in EC films

Table 2: TGA data of EC films

Formulations	T_5[a] (°C)	T_{10}[a] (°C)	T_{50}[a] (°C)	T_{max}[a] (°C)	CY_{600}[b] (%)
Pure EC	301.2	323.7	361.2	365.5	6.3
EC/DATP (90/10)	316.2	338.7	366.2	368.2	6.4
EC/DATP (70/30)	293.7	331.2	366.2	366.1	4.5
EC/DATP (50/50)	276.3	321.3	368.8	362.5	4.1

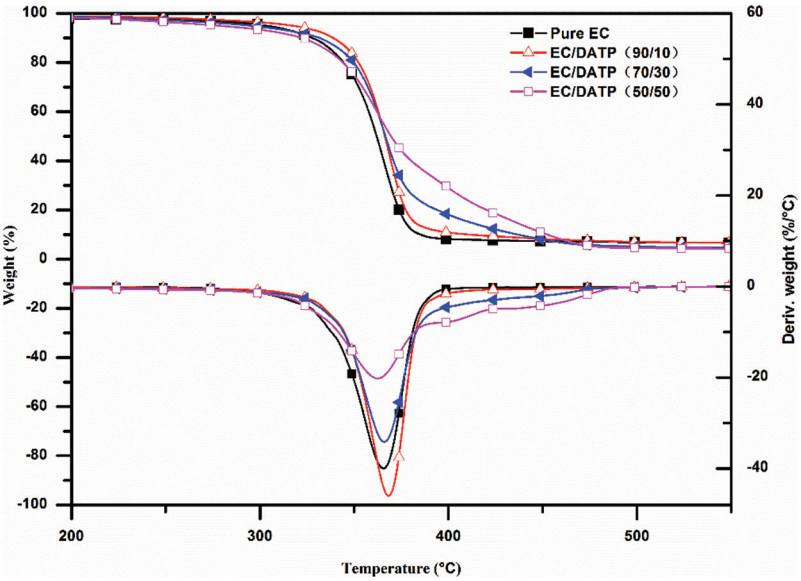

Figure 5: TGA curves of EC films

3.5 DMA

DMA was used to detect the dynamic mechanical thermal properties of the EC films. The storage modulus and loss factor (tan δ) of EC composite films are depicted in Fig. 6. The newly-formed complex compositing system consists of rigid EC units, flexible aliphatic chains, and elastic −S−. Hence, the rich DATP phase, rich EC phase, and EC/DATP phase may all exist in the compositing system. The FTIR and SEM data indicate the EC/DATP films are homogeneous.

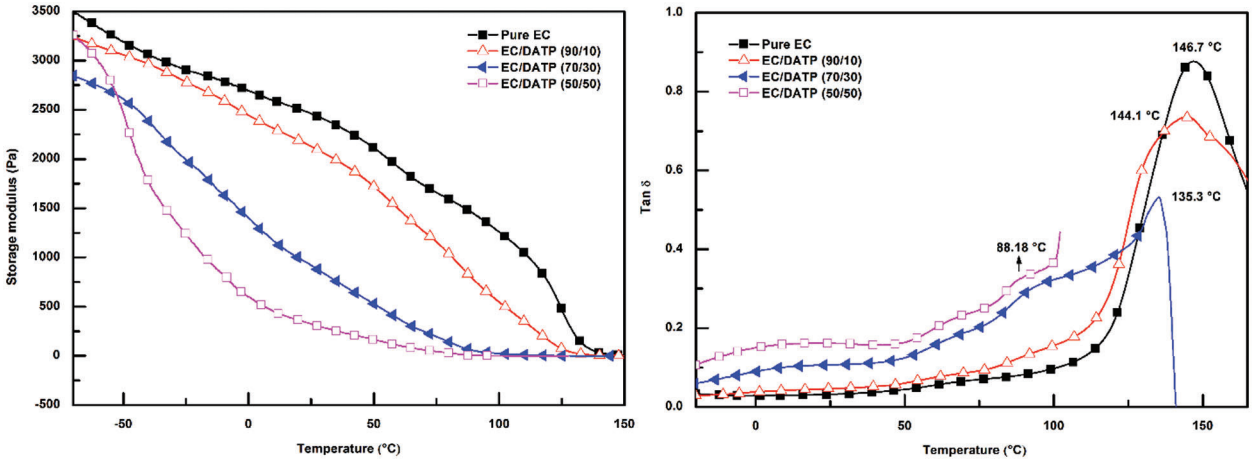

Figure 6: DMA curves of EC films

The storage modulus of all samples declines with the increasing temperature. Generally, with the presence of DATP, the storage modulus of EC films is smaller. For all composite systems, the rigid interchain hydrogen bond of pure EC is destroyed because of the addition of DATP, decreasing the storage modulus of films [33]. However, at below −50°C, the EC/DATP (50/50) system shows a

relatively higher storage modulus. The reason is that the rich DATP phase in this composite can be frozen more easily at certain temperatures.

The loss factor analysis curves become increasingly irregular with the rise of DATP content, which may be because the molecular movement of DATP in the composite system becomes freer at high temperatures. The pure EC film possesses a relatively higher T_g of 146.7°C, which is close to the data reported before [21]. The T_g of EC composite films drops from 144.1°C to 88.2°C with the increasing content of DATP. This is because the introduction of the oxhydryl, thioether, polar groups carbonyl, and long alkyl chain structures of DATP can damage the hydrogen bonding system of EC. When the temperature is near or above T_g, the supramolecular films start to creep with the structure lost, and the van der Waals force is weakened, which accounts for such a change trend on the loss factor curves.

3.6 Mechanical Properties

Fig. 7 shows the representative stress-strain curves of the composite films. The detailed mechanical properties were summarized in Table 3, including film thickness, tensile strength, elongation at break, and elastic modulus. The pure EC film has an elongation at a break of only 6.16% and thus is brittle. With the presence of DATP, the elongation at break is strengthened, but the tensile strength and elastic modulus decline. Elongations at break of EC/DATP (60/40) and EC/DATP (50/50) are up to 40.3% and 43.4%, respectively.

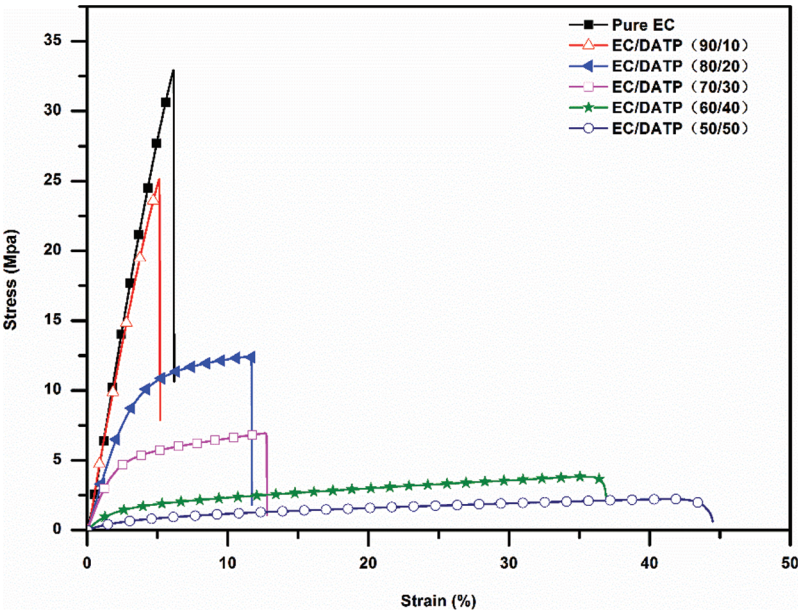

Figure 7: Stress-strain curves of different EC films

In contrast, the composite films added with 20% DATP are improved in elongation at a break from 0.77% to 2.19% [25]. Triethyl citrate and epoxidized soybean oil, two other industrial plasticizers, cannot significantly enhance the flexibility of the EC films like that [22,34]. The elongations at break of EC/STRA (60/40) and EC/STRA (50/50) increase by nearly 7.0 times from that of pure EC film.

The possible reasons are stated below. Firstly, the original hydrogen bond in EC molecular chains can be destroyed due to the introduction of DATP, and a new non-covalent bond interaction is formed between DATP and EC. Thus, a supramolecular system is established between DATP and EC [27,28]. Secondly,

the existence of elastic –S– and flexible aliphatic chains on DATP can enhance the ductility of the newly-prepared composite films [30]. Thirdly, the large atom radius and low electronegativity of sulfur result in its weak bonding with EC molecules, which can modulate the interaction of EC molecules and DATP to a suitable level.

Table 3: Mechanical properties of pure EC and EC/DATP films

Formulations	Films thickness (mm)	Tensile strength (MPa)	Elongation at break (%)	Elasticity modulus (MPa)
Pure EC	0.32	33.00 ± 1.32	6.16 ± 2.40	419.06 ± 23.25
EC/DATP (90/10)	0.21	24.07 ± 2.44	5.48 ± 0.24	426.13 ± 61.92
EC/DATP (80/20)	0.25	11.66 ± 0.32	6.53 ± 2.55	427.63 ± 38.22
EC/DATP (70/30)	0.24	7.19 ± 1.04	11.38 ± 2.63	316.00 ± 29.53
EC/DATP (60/40)	0.30	4.51 ± 0.63	40.28 ± 6.53	124.27 ± 8.44
EC/DATP (50/50)	0.40	2.32 ± 1.09	43.37 ± 4.39	42.99 ± 20.37

3.7 Contact Angle

Fig. 8 shows the contact angles of the composite films. The water contact angles of EC films (a) are ranked as: EC/DATP (100/0) [85.46°] > EC/DATP (90/10) [73.61°] > EC/DATP (70/30) [50.09°] > EC/DATP (50/50) [37.39°]. The oil contact angles of EC films (b) are ranked as: EC/DATP (100/0) [1.67°] < EC/DATP (90/10) [3.32°] < EC/DATP (70/30) [23.91°] < EC/DATP (50/50) [29.93°]. The analysis of contact angle shows that the composite films become more hydrophilic and oleophobic with more DATP added. It was because the introduction of DATP leads to an increased amount of free hydrophilic hydroxyl group on the surface of composite films. Hence, the compositing films can be used as hydrophilic films.

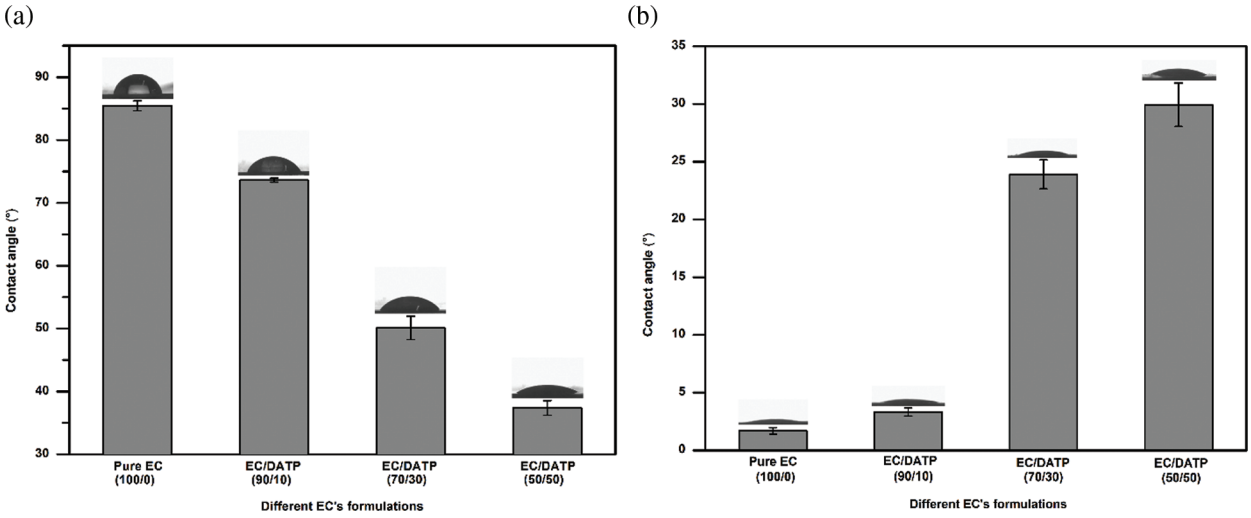

Figure 8: Contact angles of the various EC formulations

4 Conclusions

A novel special plasticizer for EC named dimer-fatty-acid-based thioether polyol (DATP) was successfully prepared, and incorporated into EC systems to form novel supramolecular composite systems. The thermal stability test demonstrates the EC/DATP (90/10) system has a higher initial temperature of thermal degradation than that of pure EC, indicating the formation of a better supramolecular system in this composite film. The incorporation of DATP strengthens the flexibility of the EC films. With the addition of DATP, the elongation at the break of EC films increases, but the tensile strength and elastic modulus decline. The elongations at break of EC/DATP (60/40) and EC/DATP (50/50) increase by nearly 7.0 times from that of pure EC film. The EC/DATP films possess a lower storage modulus and T_g than pure EC. The T_g of the EC films varies from 146.7°C to 88.2°C. In summary, these new vegetable-oil-based supramolecular cellulose films will have broad applications because of their controllable mechanical properties and flexibility. These supramolecular films can partially substitute traditional fossil-based thermoplastic films and are expected to be used in packaging, energy, chemical industry, materials, agriculture, medicine, and other fields.

Funding Statement: This work was supported by Jiangsu Province Biomass Energy and Materials Laboratory, China (Grant No. JSBEM-S-202007).

Conflicts of Interest: The authors declare that they have no conflicts of interest to report regarding the present study.

References

1. Etxabide, A., Leceta, I., Cabezudo, S., Guerrero, P., de la Caba, K. (2016). Sustainable fish gelatin films: From food processing waste to compost. *ACS Sustainable Chemistry & Engineering, 4(9),* 4626–4634. DOI 10.1021/acssuschemeng.6b00750.
2. Chen, G. Q., Patel, M. K. (2011). Plastics derived from biological sources: Present and future: A technical and environmental review. *Chemical Reviews, 112(4),* 2082–2099. DOI 10.1021/cr200162d.
3. Qin, Y., Wang, X. (2010). Carbon dioxide-based copolymers: Environmental benefits of PPC, an industrially viable catalyst. *Biotechnology Journal, 5(11),* 1164–1180. DOI 10.1002/biot.201000134.
4. Dawin, T. P., Ahmadi, Z., Taromi, F. A. (2018). Bio-based solution-cast blend films based on polylactic acid and polyhydroxybutyrate: Influence of pyromellitic dianhydride as chain extender on the morphology, dispersibility, and crystallinity. *Progress in Organic Coatings, 119,* 23–30. DOI 10.1016/j.porgcoat.2018.02.003.
5. Morales, A., Andrés, M. Á., Labidi, J., Gullón, P. (2019). UV–vis protective poly(vinyl alcohol)/bio-oil innovative films. *Industrial Crops and Products, 131,* 281–292. DOI 10.1016/j.indcrop.2019.01.071.
6. Sharma, C., Bhardwaj, N. K. (2020). Fabrication of natural-origin antibacterial nanocellulose films using bio-extracts for potential use in biomedical industry. *International Journal of Biological Macromolecules, 145,* 914–925. DOI 10.1016/j.ijbiomac.2019.09.182.
7. Suaduang, N., Ross, S., Ross, G. M., Pratumshat, S., Mahasaranon, S. (2019). Effect of spent coffee grounds filler on the physical and mechanical properties of poly(lactic acid) bio-composite films. *Materials Today: Proceedings, 17,* 2104–2110. DOI 10.1016/j.matpr.2019.06.260.
8. Landaeta, E., Schultz, Z. D., Burgos, A., Schrebler, R., Isaacs, M. (2018). Enhanced photostability of cuprous oxide by lignin films on glassy carbon electrodes in the transformation of carbon dioxide. *Green Chemistry, 20(10),* 2356–2364. DOI 10.1039/c8gc00365c.
9. Sonkaew, P., Sane, A., Suppakul, P. (2012). Antioxidant activities of curcumin and ascorbyl dipalmitate nanoparticles and their activities after incorporation into cellulose-based packaging films. *Journal of Agricultural and Food Chemistry, 60(21),* 5388–5399. DOI 10.1021/jf301311g.
10. Pelissari, F. M., Grossmann, M. V. E., Yamashita, F., Pineda, E. A. G. (2009). Antimicrobial, mechanical, and barrier properties of cassava starch−chitosan films incorporated with oregano essential oil. *Journal of Agricultural and Food Chemistry, 57(16),* 7499–7504. DOI 10.1021/jf9002363.

11. Jiang, G., Wang, G., Zhu, Y., Cheng, W., Cao, K. et al. (2022). A scalable bacterial cellulose ionogel for multisensory electronic skin. *Research, 2022,* 9814767. DOI 10.34133/2022/9814767.
12. Zhao, D., Pang, B., Zhu, Y., Cheng, W., Cao, K. et al. (2022). A stiffness-switchable, biomimetic smart material enabled by supramolecular reconfiguration. *Advanced Materials, 34(10),* 2107857. DOI 10.1002/adma.202107857.
13. Lu, Y., Yuan, W. (2017). Superhydrophobic/superoleophilic and reinforced ethyl cellulose sponges for oil/water separation: Synergistic strategies of cross-linking, carbon nanotube composite, and nanosilica modification. *ACS Applied Materials & Interfaces, 9(34),* 29167–29176. DOI 10.1021/acsami.7b09160.
14. Heredia-Guerrero, J. A., Ceseracciu, L., Guzman-Puyol, S., Paul, U. C., Alfaro-Pulido, A. et al. (2018). Antimicrobial, antioxidant, and waterproof RTV silicone-ethyl cellulose composites containing clove essential oil. *Carbohydrate Polymers, 192,* 150–158. DOI 10.1016/j.carbpol.2018.03.050.
15. Chen, J., Wu, D., Pan, K. (2016). Effects of ethyl cellulose on the crystallization and mechanical properties of poly (β-hydroxybutyrate). *International Journal of Biological Macromolecules, 88,* 120–129. DOI 10.1016/j.ijbiomac.2016.03.048.
16. Katsumura, A., Sugimura, K., Nishio, Y. (2018). Calcium carbonate mineralization in chiral mesomorphic order-retaining ethyl cellulose/poly(acrylic acid) composite films. *Polymer, 139,* 26–35. DOI 10.1016/j.polymer.2018.02.006.
17. Es-haghi, H., Mirabedini, S. M., Imani, M., Farnood, R. R. (2014). Preparation and characterization of pre-silane modified ethyl cellulose-based microcapsules containing linseed oil. *Colloids and Surfaces A: Physicochemical and Engineering Aspects, 447,* 71–80. DOI 10.1016/j.colsurfa.2014.01.021.
18. Pang, L., Gao, Z., Feng, H., Wang, S., Ma, R. et al. (2017). Synthesis of a fluorescent ethyl cellulose membrane with application in monitoring 1-naphthylacetic acid from controlled release formula. *Carbohydrate Polymers, 176,* 160–166. DOI 10.1016/j.carbpol.2017.07.057.
19. Wu, K., Zhu, Q., Qian, H., Xiao, M., Corke, H. et al. (2018). Controllable hydrophilicity-hydrophobicity and related properties of konjac glucomannan and ethyl cellulose composite films. *Food Hydrocolloids, 79,* 301–309. DOI 10.1016/j.foodhyd.2017.12.034.
20. Pottathara, Y. B., Thomas, S., Kalarikkal, N., Griesser, T., Grohens, Y. et al. (2019). UV-induced reduction of graphene oxide in cellulose nanofibril composites. *New Journal of Chemistry, 43(2),* 681–688. DOI 10.1039/c8nj03563f.
21. Lee, S., Ko, K. H., Shin, J., Kim, N. K., Kim, Y. W. et al. (2015). Effects of the addition of dimer acid alkyl esters on the properties of ethyl cellulose. *Carbohydrate Polymers, 121,* 284–294. DOI 10.1016/j.carbpol.2014.12.029.
22. Yang, D., Peng, X., Zhong, L., Cao, X., Chen, W. et al. (2014). "Green" films from renewable resources: Properties of epoxidized soybean oil plasticized ethyl cellulose films. *Carbohydrate Polymers, 103,* 198–206. DOI 10.1016/j.carbpol.2013.12.043.
23. Bueno-Ferrer, C., Garrigós, M. C., Jiménez, A. (2010). Characterization and thermal stability of poly(vinyl chloride) plasticized with epoxidized soybean oil for food packaging. *Polymer Degradation and Stability, 95(11),* 2207–2212. DOI 10.1016/j.polymdegradstab.2010.01.027.
24. Vieira, M. G. A., da Silva, M. A., dos Santos, L. O., Beppu, M. M. (2011). Natural-based plasticizers and biopolymer films: A review. *European Polymer Journal, 47(3),* 254–263. DOI 10.1016/j.eurpolymj.2010.12.011.
25. Hyppölä, R., Husson, I., Sundholm, F. (1996). Evaluation of physical properties of plasticized ethyl cellulose films cast from ethanol solution Part I. *International Journal of Pharmaceutics, 133(1–2),* 161–170. DOI 10.1016/0378-5173(96)04436-5.
26. Delbianco, M., Bharate, P., Varela-Aramburu, S., Seeberger, P. H. (2016). Carbohydrates in supramolecular chemistry. *Chemical Reviews, 116(4),* 1693–1752. DOI 10.1021/acs.chemrev.5b00516.
27. Li, M., Xia, J., Ding, C., Mao, W., Ding, H. et al. (2017). Development and characterization of ricinoleic acid-based sulfhydryl thiol and ethyl cellulose blended membranes. *Carbohydrate Polymers, 175,* 131–140. DOI 10.1016/j.carbpol.2017.07.069.
28. Lin, Y., Asante, F. O., Xu, X., Li, S., Ding, H. et al. (2020). A naturally tailored small molecule for the preparation of ethyl cellulose supramolecular composite film. *Cellulose, 28(1),* 289–300. DOI 10.1007/s10570-020-03532-9.

29. de Brabander, C., van den Mooter, G., Vervaet, C., Remon, J. P. (2002). Characterization of ibuprofen as a nontraditional plasticizer of ethyl cellulose. *Journal of Pharmaceutical Sciences, 91(7),* 1678–1685. DOI 10.1002/jps.10159.
30. Wang, Q., Cheng, M., Jiang, J. L., Wang, L. Y. (2017). Modulating the properties of quadruple hydrogen bonded supramolecular polymers by photo-cross-linking between the coumarin moieties. *Chinese Chemical Letters, 28(4),* 793–797. DOI 10.1016/j.cclet.2017.02.008.
31. Qin, H. L., Yu, H. Q. (2016). *Handbook of analyticalchemistry•7A• H-1nuclear magnetic resonance spectroscopy analysis*. 3rd edition. Beijing: Chemical Industry Press.
32. Lin, Y., Li, M., Xia, J., Ding, H., Xu, L. et al. (2021). Synthesis of plant oil derived polyols and their effects on the properties of prepared ethyl cellulose composite films. *Cellulose, 28(7),* 4211–4222. DOI 10.1007/s10570-021-03811-z.
33. Cao, S., Li, S., Li, M., Xu, L., Ding, H. et al. (2019). The thermal self-healing properties of phenolic polyurethane derived from polyphenols with different substituent groups. *Journal of Applied Polymer Science, 136(6),* 47039. DOI 10.1002/app.47039.
34. Tarvainen, M., Sutinen, R., Peltonen, S., Mikkonen, H., Maunus, J. et al. (2003). Enhanced film-forming properties for ethyl cellulose and starch acetate using n-alkenyl succinic anhydrides as novel plasticizers. *European Journal of Pharmaceutical Sciences, 19(5),* 363–371. DOI 10.1016/S0928-0987(03)0013.